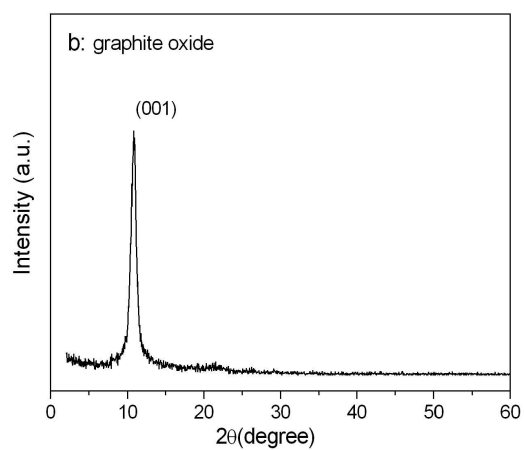
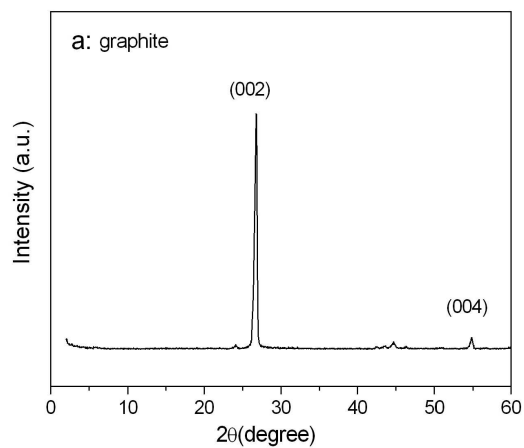


Supporting Information

Graphene-metal particle nanocomposites

Chao Xu, Xin Wang, Junwu Zhu

Key Laboratory for Soft Chemistry and Functional Materials (Nanjing University of Science and Technology), Ministry of Education, Nanjing 210094, China



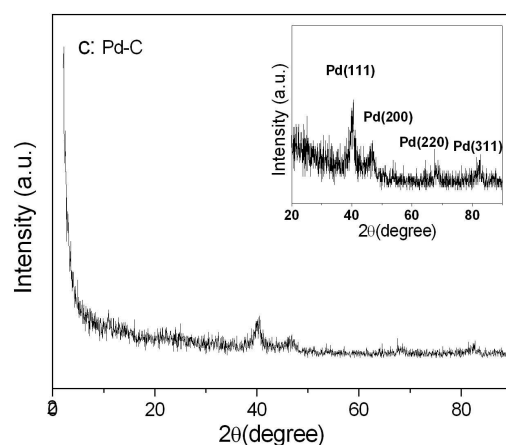


Figure 1S XRD patterns of (a) graphite, (b) graphite oxide and (c) the Pd-C composite.

Figure 1S shows the XRD patterns of the original graphite, the graphite oxide and the Pd-C composite. In Figure 1S(a), the (002) diffraction peak of graphite appeared at around $2\theta=24^\circ$, and the interlayer space was about 0.34 nm.¹ After oxidation, the interlayer space of graphite oxide (0.82 nm) was larger than that of the pure graphite, as a result of the introduction of oxygenated functional groups on carbon sheets (Figure 1S(b)). Meanwhile, the characteristic diffraction peak (001) of graphite oxide became obvious.² As shown in Figure 1S(c), the peaks at $2\theta=40.3, 46.6, 68.4,$ and 82.1° can be assigned to the (111), (200), (220), and (311) crystalline planes of Pd, respectively (JCPDS No.01-1201). However, it was worthwhile to note that, no obvious peaks attributing to graphite or graphite oxide were found in Pd-C composite, indicating the exfoliation of the layered graphite oxide.³

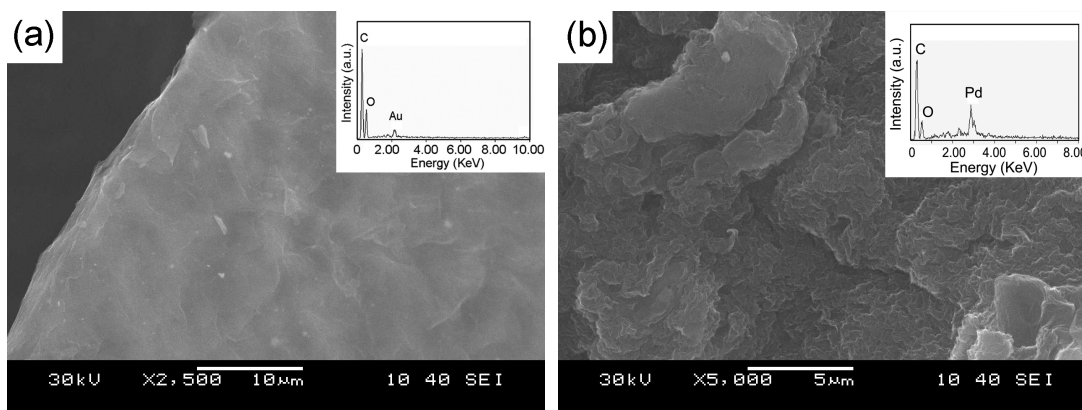


Figure 2S SEM images and EDS spectra of (a) Au-C, (b) Pd-C.

Apart from the initial element C and O, the metal elements also appeared on the surface of carbon sheets. In addition, the carbon sheets became more corrugated. As discussed in the text, it may be caused by the reduction of graphene oxide sheets.

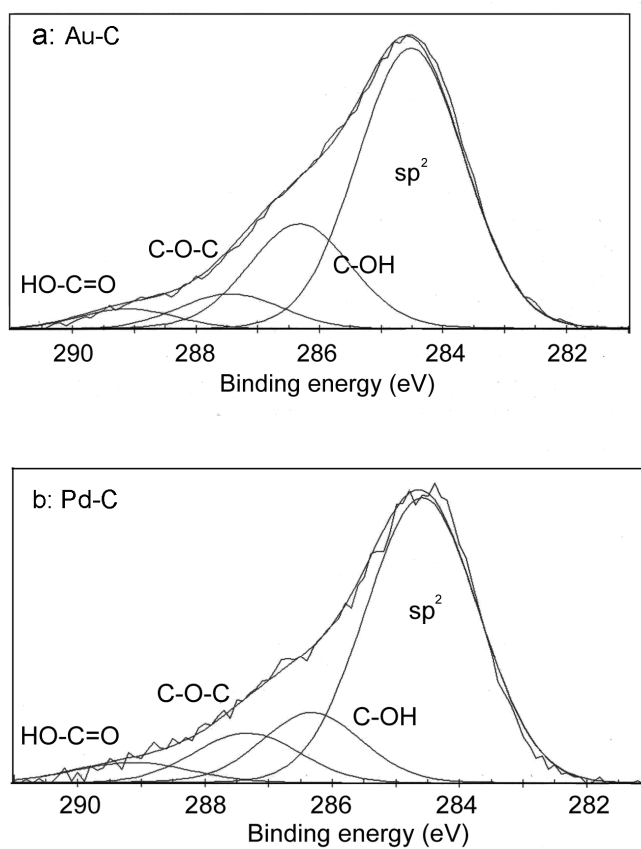


Figure 3S the C1s XPS spectra of (a) Au-C and (b) Pd-C composites.

Table 1S. XPS data of C1s of GO and Pt-C composite deconvoluted mainly into four peaks, binding energies and area percentages with respect to C-C bonds in parentheses.

samples	C-C	C-OH	C-O-C	HO-C=O
GO	284.86 (100)	286.19 (28)	287.57 (59)	289.24 (11)
Pt-C	284.52 (100)	286.30 (19)	287.53 (14)	289.13 (6)
Au-C	284.52 (100)	286.32 (27)	287.44 (12)	289.11 (6)
Pd-C	284.59 (100)	286.32 (22)	287.34 (16)	289.14 (7)

It was found that four kinds oxygenated functional groups appeared in the graphene oxide sheets (Table 1S). After reduced by ethylene glycol, the content changes of these groups took place in these reduced graphene oxide sheets. Specially, the epoxy groups obviously decreased, and the hydroxyl groups, especially in Pt-C composite, also become weak. The difference in de-oxygenation extent of oxygenated functional groups resulted from the diversified catalysis activity between the attached metal NPs.

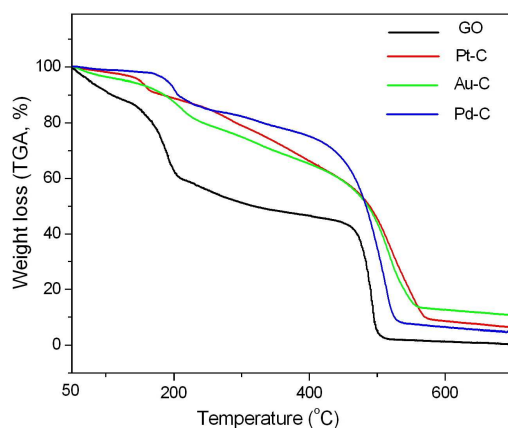


Figure 4S TGA curves of graphite oxide, Au-C, Pt-C and Pd-C composites.

GO is thermally unstable and starts to lose mass upon heating below 100 °C due to

the adsorbed water. There are two significant drops in mass around 215 and 550 °C. The former is assigned to the evolution of CO and CO₂ from GO caused by the destruction of oxygenated functional groups, and the latter is attributed to the combustion of the carbon skeleton of GO. It was found that the weight loss at around 200 °C in the as-synthesized nanocomposites were much lower than that of the original ones, indicating the decreased of oxygenated functional groups.

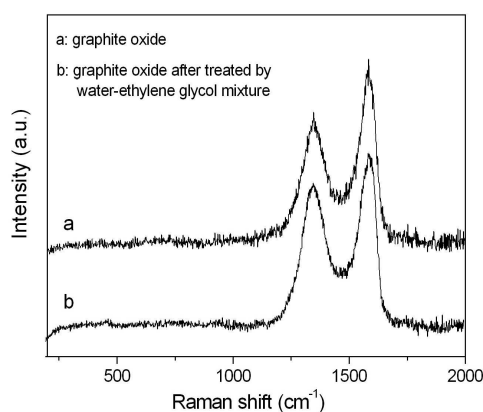


Figure 5S The Raman spectrum of graphite oxide collected in water-ethylene glycol mixture.

Figure 5S displays the graphite oxide and the sample collected after treated by water-ethylene glycol without metallic salts (labeled as GO-EG). By comparison, the spectrum of GO-EG was similar to that of the starting graphite oxide, but different from that of carbon sheets in composites, indicating that no reductive reaction happened in the GO-EG system.

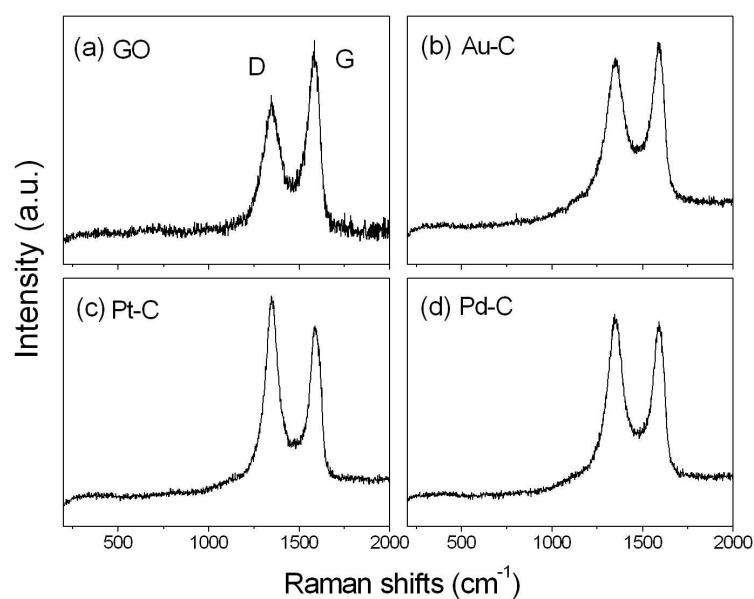


Figure 6S The Raman spectra of (a) graphite, (b) Au-C, (c) Pt-C and (d) Pd-C.

In the Raman spectrum of graphene oxide, two prominent peaks D (1355 cm^{-1}) and G (1598 cm^{-1}) appeared which were usually assigned to the breathing mode of κ -point phonons of A_{1g} symmetry and the E_{2g} phonon of C sp^2 atoms, respectively.⁴ After chemical reduction of graphene oxide, the intensity ratio of D/G will be changed. It is known that intensity ratio of D/G was proportional to the reciprocal of the average crystallite size in graphite materials. As demonstrated in some research, the oxygen functional groups in graphene oxide sheets can be removed by chemical reduction, and the conjugated graphene network (sp^2 carbon) will be reestablished.⁵ However, the size of the reestablished graphene network was smaller than the original ones, which lead to the increase of intensity ratio of the D/G consequently.⁶ The changes of the intensity ratio of D/G can also be found in our system. As shown in Figure 6S, the D/G ratios of these composites were higher than that of starting graphene oxide, especially in the Pt-C

composite. Such phenomena could be attributed to the reducing action of the ethylene glycol on graphene oxide. Additionally, we found that the appearance of these metal particles on graphene oxide sheets played catalysis on the reduction of graphene oxide with ethylene glycol. However, the catalysis activities of these metals were different from each other. Thus, the difference of the D/G ratio can be found in the Raman spectra.

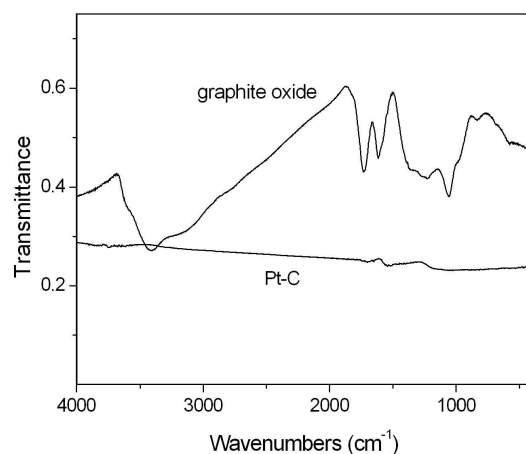


Figure 7S FT-IR spectra of graphite oxide and Pt-C composite.

The characteristic features in the FT-IR spectrum of graphite oxide are the absorption bands corresponding to the C=O carbonyl stretching at 1720 cm⁻¹, the C-OH stretching at 1224 cm⁻¹, and the C-O stretching at 1050 cm⁻¹.^{7,8} The spectrum also shows a C=C peak at 1620 cm⁻¹ corresponding to the remaining sp² character.⁹ After reduced by ethylene glycol, most of the functional groups were removed. Given that carboxylic acid groups are unlikely to be reduced under the given reaction conditions, these groups should therefore remain in the reduced product as confirmed by our FT-IR analysis. The absorption band at around 1,700 cm⁻¹ is attributed to carboxyl groups.¹⁰ The absorption of Pt-C at this range is observable but not as prominent as that observed for graphite

oxide, likely due to the overlapping of the strong absorption of graphene sheets in this region.

References

- (1) Bourlinos, A. B.; Gournis, D.; Petridis, D.; Szabó, T.; Szeri, A.; Dékány, I. *Langmuir* 2003, 19, 6050.
- (2) Jeong, H. K.; Lee, Y.P.; Lahaye, R.; Park, M.; An, K. H.; Kim, I. J.; Yang, C.; Park, C. Y.; Ruoff, R. S.; Lee, Y. H. *J. Am. Chem. Soc.* **2008**, 130, 1362.
- (3) Cai, D.Y.; Song, M. *J. Mater. Chem.* **2007**, 17, 3678.
- (4) Tuinstra, F.; Koenig, J. L. *J. Chem. Phys.* **1970**, 53, 1126.
- (5) Stankovich, S. Dikin, D. A.; Piner, R. D.; Kohlhaas, K. A.; Kleinhammes, A.; Jia, Y.; Wu, Y.; Nguyen, S. T.; Ruoff, R. S. *Carbon* **2007**, 45, 1558.
- (6) Wang, G.; Yang, J.; Park, J.; Gou, X.; Wang, B.; Liu, H.; Yao, J. *J. Phys. Chem. C* **2008**, 112, 8192.
- (7) Matsuo, Y.; Miyabe, T.; Fukutsuka, T.; Sugie, Y. *Carbon* **2007**, 45, 1005.
- (8) Kovtyukhova, N. I.; Ollivier, P. J.; Martin, B. R.; Mallouk, T. E.; Chizhik, S. A.; Buzaneva, E. V.; Gorchinskiy, A. D.
- (9) Herrera-Alonso, M.; Abdala, A. A.; McAllister, M. J.; Aksay, I. A.; Prud'homme, R.K. *Langmuir* **2007**, 23, 10644.
- (10) Li, D.; Müller, M. B.; Gilje, S.; Kaner, R. B.; Wallace, G. G. *Nature Nanotechnol.* **2007**, 3, 101.